Calving Speed of Alaska Tidewater Glaciers, With Application to Columbia Glacier

GEOLOGICAL SURVEY PROFESSIONAL PAPER 1258–C

Calving Speed of Alaska Tidewater Glaciers, With Application to Columbia Glacier

By C. S. BROWN, M. F. MEIER, *and* AUSTIN POST

STUDIES OF COLUMBIA GLACIER, ALASKA

GEOLOGICAL SURVEY PROFESSIONAL PAPER 1258-C

A study of 15 iceberg-calving glaciers in Alaska establishes a relation between calving speed and water depth at the terminus

UNITED STATES GOVERNMENT PRINTING OFFICE, WASHINGTON:1982

UNITED STATES DEPARTMENT OF THE INTERIOR

JAMES G. WATT, *Secretary*

GEOLOGICAL SURVEY

Dallas L. Peck, *Director*

Library of Congress catalog-card No. 82-600559

**For sale by the Distribution Branch, U.S. Geological Survey,
604 South Pickett Street, Alexandria, VA 22304**

CONTENTS

ILLUSTRATIONS

[Plates are in pocket]

TABLES

SYMBOLS AND ABBREVIATIONS

Symbol	Name	Unit (where applicable)
A	Glacier surface area	km^2
a	Year.	
α	Surface slope	dimensionless
$\dot{b}$	Balance rate	m/a
c	Calving coefficient	*
D	Short-term runoff at the terminus	m^3/s
d	Calving coefficient	a^{-1}
e_h	Standard error in h or h_w	dimensionless
e_v	Standard error in v_c	dimensionless
F	Variance reduction fraction	dimensionless
g	Acceleration due to gravity	km/a^2
h	Glacier thickness	m
$\dot{h}$	Time rate of change in surface altitude, positive when thickening	m/a
h_g	Ice cliff height	m
h_u	Ice thickness not supported by buoyancy	m
h_w	Water depth at the terminus	m
km	Kilometer.	
m	Meter.	
p	Calving coefficient	dimensionless
Φ	Calving relation	*
Q	Glacier flux	m^3/a
Q_b	Balance flux	m^3/a
Q_c	Calving flux	m^3/a
Q_h	Thickness change flux	m^3/a
q	Calving coefficient	dimensionless
ρ_i	Density of ice.	
ρ_w	Density of water.	
S	Area of glacier cross section	km^2
$\hat{S}$	Area of vertical projection of the glacier surface	km^2
S'	Area between a given contour line at the beginning and end of a period of observation	km^2
s	Shape factor	dimensionless
σ_c	Standard error of estimate of c	*
T	Total time in period of observation	a
t	Time	a
τ	Basal shear stress	bar
V	Volume of glacier	km^3
v	Glacier surface speed at the terminus	m/a
v_c	Calving speed	m/a
W	Glacier width	km
X	Terminus position	km
$\dot{X}$	**Time rate of change of terminus position, positive when advancing**	m/a
x	Horizontal coordinate, positive in direction of flow	km
y	Distance from centerline on a horizontal line perpendicular to the flow	m
z	Vertical coordinate, positive upwards (altitude)	m
z_m	Highest altitude of glacier	m
z_n	Highest altitude at which thinning occurred	m

* Dimensions depend on form of the calving relation.

STUDIES OF COLUMBIA GLACIER, ALASKA

CALVING SPEED OF ALASKA TIDEWATER GLACIERS, WITH APPLICATION TO COLUMBIA GLACIER

By C. S. BROWN, M. F. MEIER, and AUSTIN POST

ABSTRACT

Columbia Glacier is a grounded, tidewater glacier, 1,100 km² in area, which actively calves icebergs from its terminus. Calving speed, defined as the volume rate of iceberg discharge from the terminus divided by the cross-sectional area of the terminus, depends on measurable properties of the terminus; this relation forms the terminus boundary condition for predictive models. Calving speed is the difference between glacier speed and the rate of terminus advance. The mean yearly calving speed calculated in this way for 12 glaciers in Alaska ranges from 220 to 3,700 m/a. Yearly calving speeds estimated by using balance flux and thinning flux for three additional glaciers that recently underwent rapid retreat extend the range of calving speed to 12,500 m/a. A statistical analysis of calving speed and mean yearly values for water depth, cliff height, and glacier thickness at the terminus indicates that calving speed is fit best by a simple proportionality to average water depth at the terminus, with a constant of proportionality equal to 27 a^{-1}, producing a variance reduction fraction of 0.90. This calving relation uses mean yearly values. A proposed seasonal calving relation, which involves runoff as a variable, does not appear to be compatible.

INTRODUCTION

Nearly all grounded, iceberg-calving glaciers in Alaska have undergone large-scale asynchronous advances and retreats. This behavior apparently is not related directly to climatic variations. The water depth at the terminus appears to be a critical factor; instability results when a calving glacier retreats from a shoal so that its terminus is in contact with deeper water. The glacier may retreat rapidly and irreversibly as the rate of iceberg calving increases greatly (Post, 1975).

Columbia Glacier, near Valdez, Alaska (fig. 1), is a large calving glacier; it is 67 km long and 1,100 km² in area. It now ends on a moraine shoal in shallow water, but, upglacier from the terminus, the bed is about 400 m below sea level. The glacier is grounded throughout except for some small areas associated with ice-dammed lakes; none of the tidewater terminus is floating. Although the position of the terminus has been at near equilibrium since 1794, evidence now suggests that rapid, drastic retreat may be imminent (Post, 1975). Small icebergs drift from Columbia Glacier toward and occasionally into Valdez Arm (fig. 1). Drastic retreat would substantially increase the discharge of ice and thus would increase hazard to shipping. To determine when this retreat and increased discharge might happen and how much the iceberg discharge would be increased, an intensive study was begun by the U.S. Geological Survey in 1977, and a preliminary prediction was issued in 1980 (Meier and others, 1980a).

This report is the third in a series of papers publishing the scientific results of this study. Other papers in the series discuss photogrammetric derivation of ice velocity and thickness change; mass balance observations; field measurements of velocity, thickness, and thickness change; the adjustment and interpolation of point data; a continuity model of the terminus retreat and the rate of iceberg discharge (Rasmussen and Meier, 1982); a finite element model of the flow of the lower glacier (Sikonia, 1982); and several additional topics.

Development of the continuity model required knowledge of the rate of ice flow to the terminus of a calving glacier and of the rate of ice loss by calving from the terminus. The ice flow cannot be analyzed as a conventional problem in glacier-flow dynamics because the location and the geometry of the terminus depend on the rate of iceberg calving. A calving relation that gives the rate of calving as a function of certain characteristics of the terminus must be used as the terminus boundary condition for the ice flow analysis. A calving relation also is needed that would provide estimates of future iceberg discharge. This relation would have to be valid for deeper water and other aspects of a changed glacier geometry. This report describes the development of the

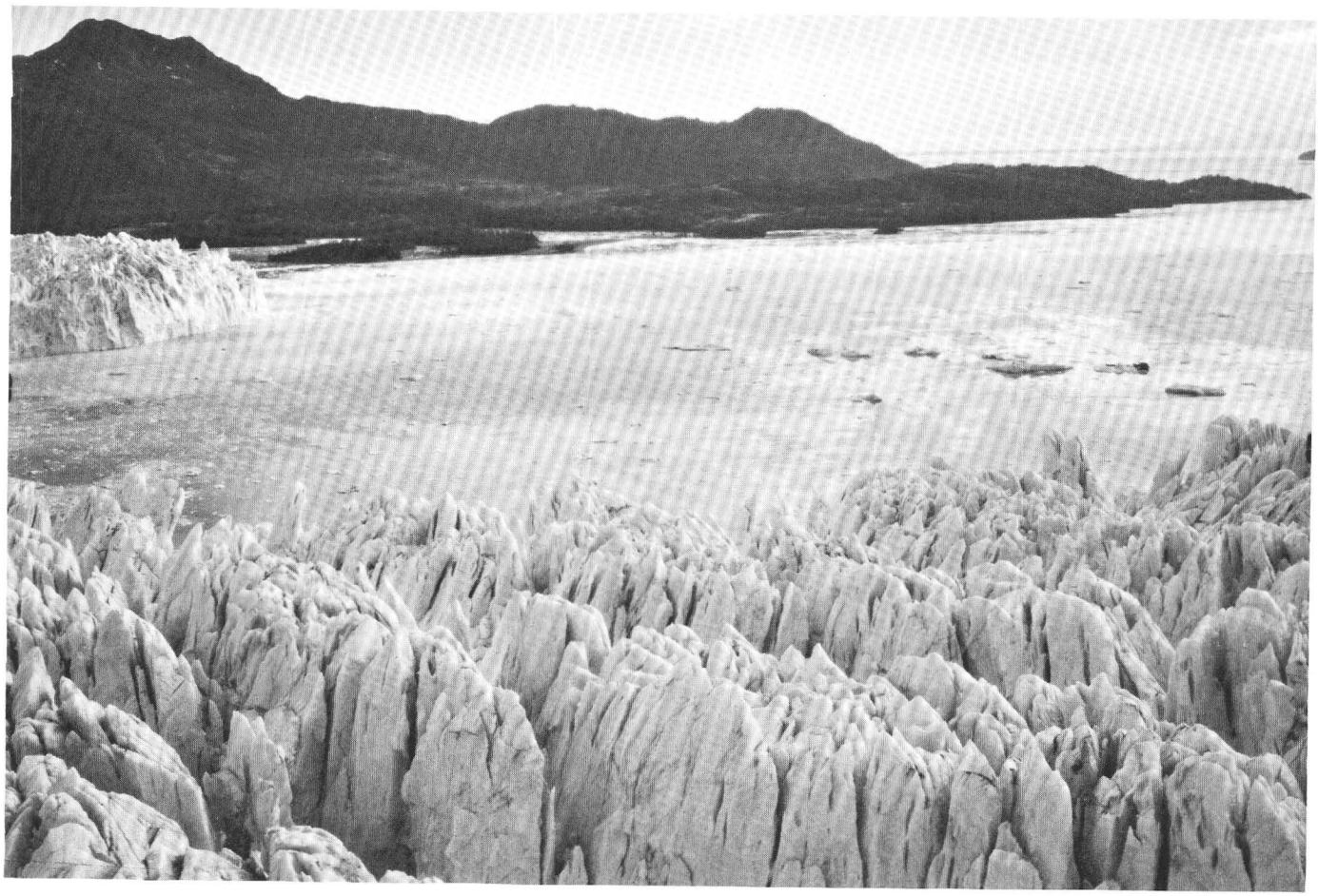

FIGURE 1.—Terminus of Columbia Glacier, Alaska, a typical grounded, iceberg-calving glacier. The wide embayment in the ice front is typical of this glacier. For scale, this embayment is about 1.5 km wide, and the ice cliff stands about 90 m above the sea. The surface of Columbia Bay is choked with many small ice fragments and several larger icebergs that drift around the ridge in the background through the gap to the far right and, from there, into Valdez Arm. (Aerial photograph by L. R. Mayo, Oct. 8, 1975; view facing southeast.)

annually averaged calving relation used in the continuity model that was developed for the prediction of the retreat of Columbia Glacier and the expected rate of iceberg discharge (Rasmussen and Meier, 1982). Very little was known about the calving relation for a grounded tidewater glacier prior to this study. The elastic strains in a grounded, calving ice block were analyzed by Iken (1977), but these results cannot be used to predict the calving rate of Columbia Glacier.

CALVING SPEED

The continuity equation for the terminus (Meier and others, 1980b) is written

$$S\dot{\bar{X}} = Q - Q_c \tag{1}$$

where $\dot{\bar{X}}$ is the time rate of change of the width-averaged position of the terminus X on the x axis, which is horizontal and positive in the direction of the flow with $x = 0$ at the head of the glacier; S is the area of the projection of the terminus onto a vertical plane normal to the x axis; Q is the volume flux of ice in the x direction to the terminus (m^3/a); and Q_c is the iceberg calving volume flux in the same direction from the terminus (m^3/a). Values averaged over the width are designated with a bar superscript; the absence of a bar superscript designates a centerline or maximum value. The ratios $Q/S \equiv \bar{v}$ and $Q_c/S \equiv \bar{v}_c$ are defined to be the average glacier speed at the terminus and the calving speed, respectively. Thus, equation 1 can be written

$$\bar{v}_c = \bar{v} - \dot{\bar{X}} \tag{2}$$

This $\bar{v}_c$ then is examined as a possible function of geometrical or other measurable properties of the terminus.

During the field seasons of 1977, 1978, and 1979, the Survey's research vessel *Growler* and the radio-controlled skiff *Bergy Bit* were used to collect data on water depth at the termini of 45 tidewater iceberg-

calving glaciers in Alaska and in the bays and fiords formerly occupied by these glaciers (Post, 1980a–f). These observational data show that all glaciers with stable, slowly advancing, or slowly retreating termini ($|\dot{\bar{X}}| < 50$ m/a) end in shallow water, generally less than 80 m deep. Conversely, all glaciers that are, or were, retreating rapidly ($0.5 < -\dot{\bar{X}} < 10$ km/a) end in water more than 80 m deep, and, in general, the deeper the water, the faster the retreat (Post, 1975; Meier and others, 1980b). The rate of retreat is a function of the rate of calving, and the rate of calving appears to be related mainly to average water depth, $\bar{h}_w$.

DIRECT DETERMINATION OF CALVING SPEED

The calving speed may be obtained from measurements of v and $\dot{X}$ using equation 2. To derive a calving relation, geometrical properties such as cliff height ($\bar{h}_s$), water depth ($\bar{h}_w$), and cross section area (S) must be measured. Data sets containing all of these variables were obtained for 12 major calving glaciers in Alaska (fig. 2): McCarty Glacier on the Kenai Peninsula, Harvard and Yale Glaciers in College Fiord, Meares Glacier in Unakwik Inlet, Columbia Glacier in Columbia Bay, Tyndall Glacier in Icy Bay, Hubbard Glacier north of Yakutat, Grand Pacific and Margerie Glaciers in Tarr Inlet of Glacier Bay, Johns Hopkins Glacier in west Glacier Bay, Muir Glacier in Muir Inlet of Glacier Bay, and South Sawyer Glacier in Tracy Arm. Table 1 lists the glaciers and the corresponding values of the variables. Tables 2 through 5 give the years or years for which the variables were measured (or the date of the photography for each glacier) and the method of measurement. Plate 1 illustrates the terminus change, the velocity measurements, and water depth at the terminus for most of the glaciers. The hydrographic data used for many of these glaciers have been published (Post, 1975, 1980a–f).

All the variables for an individual glacier should be measured in the same year, but this was not always possible; for most glaciers, all variables were measured within a 2-year period. Because there are many glaciers in Alaska and only a sparse data-collection network, there are a few instances where the time interval is considerably greater than 2 years. The largest time discrepancy occurs in using $\dot{\bar{X}}$ values determined from retreats of 10 or more years ago (McCarty Glacier, 1964–65; Tyndall Glacier, 1964–65; Grand Pacific Glacier, 1968–70; and South Sawyer Glacier, 1970–71) with recent speed and bathymetric measurements (1977–79). The water depths are judged to have changed very little at the glacier termini between the dates used to determine retreat and the date of the sounding measurements. However, the nonsynchronous $\bar{v}$ and $\dot{\bar{X}}$ measurements from South Sawyer Glacier, especially, do introduce error, because neither variable is constant in time. Using short time intervals to determine speed values also introduces error because speed varies

TABLE 1.—*Water depths* (h_w *and* $\bar{h}_w$), *ice surface height* (h_s *and* $\bar{h}_s$), *width* ($\bar{W}$), *surface area* (A), *velocities* (v *and* $\bar{v}$), *calving speed* ($\bar{v}_c$), *and rate of advance* ($\dot{\bar{X}}$) *at the terminus of 12 Alaska glaciers*

[Value given above; standard error given in parentheses. Standard error determined or estimated from precision and density of measurements, possible lack of synchronism between different measurements, and, in case of ice speed, estimated seasonal or short-term speed fluctuations compared with time interval of measurement. Glacier locations are shown in figure 2]

Number	Glacier name	h_w (m)	$\bar{h}_w$ (m)	h_s (m)	$\bar{h}_s$ (m)	$\bar{W}$ (m)	A (km²)	$\dot{\bar{X}}$ (m/a)	v (m/a)	$\bar{v}$ (m/a)	$\bar{v}_c$ (m/a)
1	McCarty	14	12	32	30	900	110	0	850	600	600
		(5)	(2)	(10)	(10)		(5)	(2)	(200)	(250)	(250)
2	Harvard	57	36	72	68	2,380	580	+10	1,560	1,090	1,080
		(5)	(5)	(10)	(10)		(50)	(2)	(470)	(400)	(400)
3	Yale	201	153	85	69	1,230	196	−440	3,600	3,060	3,500
		(20)	(25)	(10)	(10)		(15)	(10)	(900)	(700)	(800)
4	Meares	63	31	74	59	1,440	154	−34	1,390	975	1,010
		(2)	(2)	(10)	(10)		(12)	(2)	(350)	(265)	(270)
5	Columbia	134	75	90	86	4,000	1,070	−45	3,160	2,140	2,185
		(17)	(6)	(4)	(3)		(55)	(5)	(50)	(100)	(100)
6	Tyndall	100	64	52	49	2,580	48	−210	2,200	1,530	1,740
		(8)	(10)	(10)	(10)		(85)	(10)	(220)	(150)	(170)
7	Hubbard	100	80	120	92	5,500	3,910	−32	3,320	2,600	2,630
		(20)	(20)	(20)	(20)		(310)	(5)	(265)	(200)	(200)
8	Grand Pacific	34	18	47	44	1,900	660	+28	310	248	220
		(8)	(10)	(8)	(7)		(50)	(2)	(75)	(75)	(70)
9	Margerie	34	15	64	60	1,840	220	0	660	463	463
		(8)	(8)	(10)	(10)		(20)	(2)	(125)	(100)	(100)
10	Johns Hopkins	84	56	74	70	1,510	320	−50	3,180	2,240	2,290
		(2)	(2)	(10)	(13)		(25)	(2)	(1,100)	(780)	(800)
11	Muir	137	100	64	60	900	140	−600	4,450	3,100	3,700
		(10)	(10)	(7)	(10)		(10)	(12)	(2,225)	(1,550)	(2,000)
12	South Sawyer	220	186	51	48	1,140	730	−1,500	2,365	1,700	3,200
		(30)	(30)	(10)	(10)		(60)	(1,000)	(600)	(500)	(1,000)

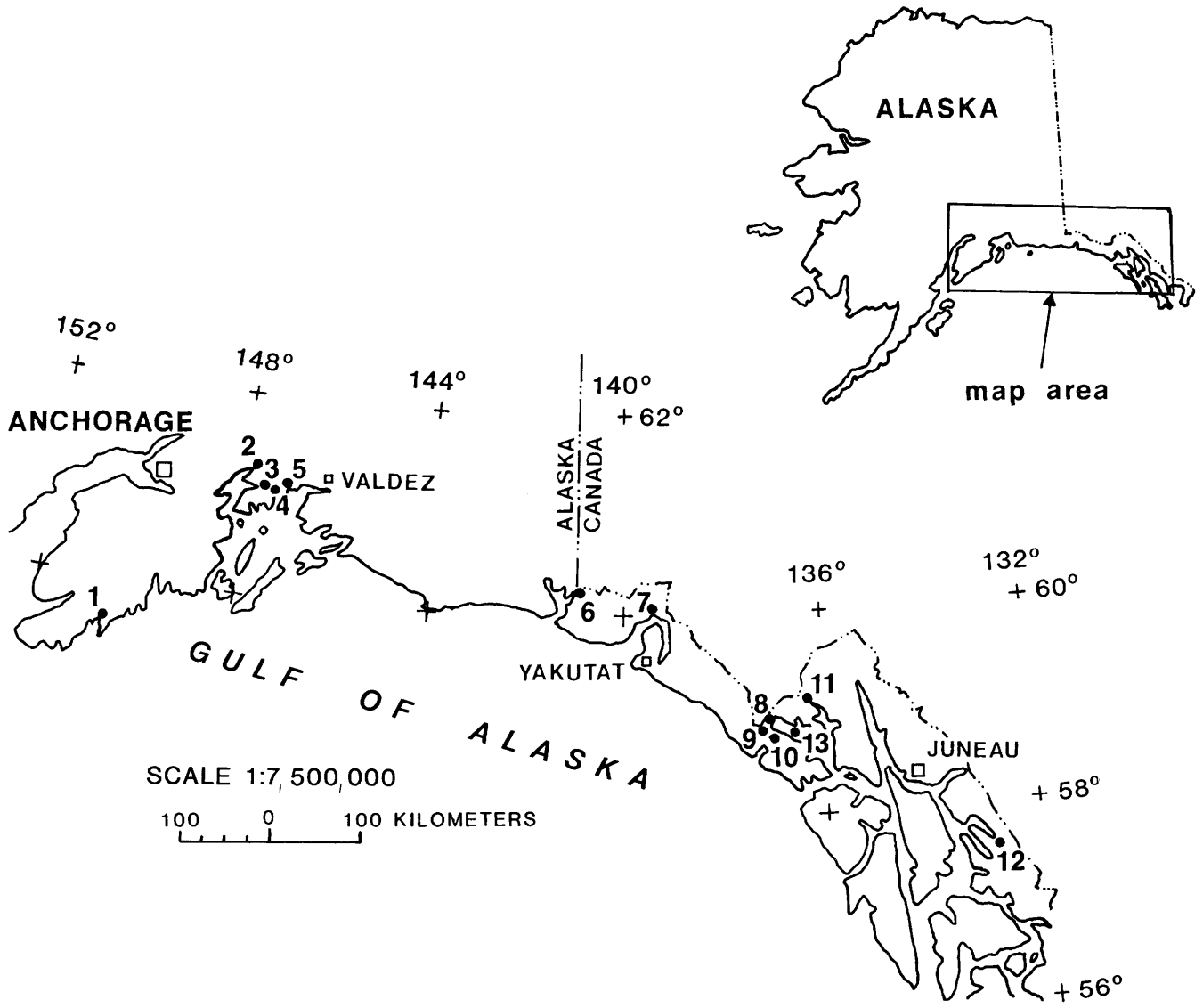

FIGURE 2.—Index map of south-central and southeastern Alaska showing the location of the 13 calving glaciers considered in this study. The numbers refer to glaciers listed in tables 1 and 6.

seasonally. Speed values were not extrapolated to the calving terminus. All these sources of error are taken into account in the statistical analyses by weighting the data inversely according to the estimated standard error squared.

Surface ice speed could not be measured across the complete width of the terminus for all glaciers. For some glaciers, only centerline values were obtained; for others, values were measured in a band across the middle of the width of the glacier. To estimate the speed averaged over the width, data were selected from the five glaciers for which speed was known as a function of width. These data were plotted on a graph of normalized speed $v/\bar{v}$ versus width-fraction $2y/W$, where the speed v occurs at distance y from the centerline and $W/2$ is the half width. A smooth curve was drawn through the points, and the integral of this curve with respect to width then was used to relate the average speed over the whole width to the average speed over a partial width or, in some cases, to a single measurement not on the centerline.

DETERMINATION OF CALVING SPEED IN THE ABSENCE OF FLOW MEASUREMENTS

Of the 12 glaciers for which a complete data set was obtained, the maximum water depth at the terminus was 220 m, and the maximum calving speed was 3,700 m/a. Future retreat of Columbia will place the terminus

TABLE 2.—*Date and method of determining water depths* $\bar{h}_w$ *and* h_w

Glacier	Date		Method
McCarty	July	1977	[1]1
Harvard	August	1978	1
Yale	August	1978	1
Meares	August	1977	1
Columbia	July–August	1977	1
Tyndall	–	1976	[2]2
Hubbard	May	1977	1 and 2
Grand Pacific	September	1978	1
Margerie	September	1978	1
Johns Hopkins	September	1978	1
Muir	July–September	1978	1
South Sawyer	August	1979	1

[1] Soundings by U.S. Geological Survey with the USGS/RV *Growler*.
[2] Soundings by National Oceanic and Atmospheric Administration.

TABLE 3.—*Method of detemining ice cliff heights* h_s *and* $\bar{h}_s$. *All photographs were taken during 1977–78 summer photo flights unless otherwise stated*

Glacier	Date	Method
McCarty	8/25/64	[1]1
Harvard		[2]2
Yale		2
Meares		2
Columbia	10/1/77–9/31/78	[3]3
Tyndall	1979	1
Hubbard		2
Grand Pacific		2
Margerie		2
Johns Hopkins		2
Muir		2
South Sawyer		2

[1] Determined from trim lines in aerial photographs.
[2] Determined by parallax measurements from contact prints of aerial photography.
[3] Determined by photogrammetric plotting (written commun., 1981).

TABLE 4.—*Method of determining surface speeds* v *and (or)* $\bar{v}$ *and dates of photographs used for measurements*

Glacier	Date	Method
McCarty	8/64–8/65	[1]1
Harvard	6/21/78–9/1/78	[2]2
Yale	7/15/77–9/3/77	2
Meares	7/15/77–9/3/77	2
Columbia	10/1/77–9/31/78	[3]3
Tyndall	8/64–8/65	[4]4
Hubbard	8/20/77–10/1/77	[5]5
Grand Pacific	8/68–7/70	4
Margerie	7/17/77–9/1/77	2
Johns Hopkins	7/17/77–9/1/77	2
Muir	8/22/79–8/26/79	2
South Sawyer	7/12/77–8/30/77	2

[1] v determined from oblique photographs using dark debris band approximately in center of glacier; debris positions located on topographic map and distances measured.
[2] v measured by Robert Krimmel (1978) from manual superposition of large-scale (~1:10,000) mylar transparencies of vertical air photographs.
[3] v determined by photogrammetry (M. F. Meier and others, written commun., 1981).
[4] v determined from measurements of two rock trajectories located on vertical photographs.
[5] v and $\bar{v}$ measured by David Frank (1978) from manual superposition of large-scale (~1:20,000) mylar transparencies of vertical air photographs.

in water depths exceeding 400 m; observations of rapidly retreating glaciers suggest that the calving speed will then greatly exceed 3,700 m/a. Therefore, an attempt was made to extend the range of the results by examining glaciers in a rapid-retreat mode. No flow measure-

TABLE 5.—*Method of determining rate of advance* $\dot{\bar{X}}$ *and dates of photographs used for measurements*

Glacier	Date	Method
McCarty	1964 to present	[1]1
Harvard	9/3/77–9/1/78	[2]2
Yale	9/3/77–9/1/78	2
Meares	9/3/77–9/1/78	2
Columbia	10/1/77–9/31/78	[3]3
Tyndall	8/64–8/65	[4]4
Hubbard	8/20/77–9/2/78	[5]5
Grand Pacific	8/68–7/70	4
Margerie	7/17/77–6/21/78	2
Johns Hopkins	9/1/77–9/3/78	2
Muir	8/78–9/79	1
South Sawyer	1970–71	2

[1] Photographs and personal observations of Austin Post (1964–1981).
[2] Manual superposition of large-scale (~1:10,000) mylar transparencies of vertical air photographs.
[3] $\dot{\bar{X}}$ determined by photogrammetry (M. F. Meier and others, written commun., 1981).
[4] Comparison of vertical photographs.
[5] Manual superposition of large-scale (1:20,000) mylar transparencies of vertical air photographs.

ments were made during these periods of rapid retreat, so it was necessary to make an indirect calculation of ice flow speed, from which calving speed could be obtained.

Two well-documented rapid retreats of glaciers are those for Muir Glacier, 1892–1972 (Reid, 1896; Field, 1947, 1975), and for McCarty Glacier, 1942–50 (Post, 1980d). Surface speed data were unobtainable, but $\dot{\bar{X}}$ could be calculated readily from two or more past terminus positions. The following method was devised to estimate $\bar{v}$ and thus calculate $\bar{v}_c$ by using equation 2 for the particular time period for which $\dot{\bar{X}}$ was known. Three maps of Muir Glacier are available, so this glacier was analyzed separately for the two periods between maps, 1892–1948 and 1948–72.

The continuity equation integrated over the entire glacier surface can be written as

$$\int_0^x (\dot{b} - \dot{h}) W dx = Q \qquad (3)$$

where $\dot{b}$ is the balance rate in meters of ice equivalent per year) and $\dot{h}$ is the time rate of change of the surface altitude (in meters of ice equivalent per year, positive in the case of thickening), both measured in the vertical; W is the width; and $x=0$ at the head of the glacier. The quantities $\dot{b}$, $\dot{h}$, and W are treated as functions of x by taking $\dot{b}$ and $\dot{h}$ at each x to be averages over W. The integral in equation 3 can be partitioned into the sum of the balance flux, Q_b, and the thickness change flux, Q_h,

$$Q = \int_0^x W\dot{b}dx + \left(-\int_0^x W\dot{h}dx\right) = Q_b + Q_h \qquad (4)$$

Then, using the ratio $Q/S = \bar{v}$, equation 4 can be rewritten

$$\bar{v} = (Q_b + Q_h)/S. \quad (5)$$

Thus, if Q_b and Q_h can be obtained, $\bar{v}$ can be determined.

The balance flux, Q_b, is determined from

$$Q_b = \sum_{i=1}^{m-1} \dot{b}(z_{i+1/2})\, \hat{S}_{i+1/2}\, \Delta z \quad (6)$$

where z is a vertical coordinate positive upwards, $z_{i+1} = z + \Delta z$ and $z_{i+1/2} = z_i + \Delta z/2$, z_m is the highest altitude on the glacier, $z_1 = h_g$, and $\hat{S}_{i+1/2}$ is the area of a vertical projection of the glacier surface between z_i and z_{i+1} (fig. 3). The average Q_b over the time interval of measurement then is taken to be the average of the integral evaluated at the beginning of the period of observation (time $t = 0$) and at the end of the period of observation ($t = T$).

The only available $\dot{b}(z)$ data for maritime glaciers in south-central Alaska are those collected at Wolverine Glacier on the Kenai Peninsula from 1966 to the present and at Columbia Glacier in Prince William Sound from 1977 to the present by L. R. Mayo and D. C. Trabant (personal commun., 1980). On the basis of the balance data from these two glaciers, examination of average runoff from nearby basins, aerial photographs, and consideration of topography and exposure to primary moisture sources, Mayo and Trabant (written commun., 1979) estimated a $\dot{b}(z)$ function for McCarty Glacier for the period 1942–60. The $\dot{b}(z)$ curve used for Muir 1892, 1948, and 1972 was the McCarty $\dot{b}(z)$ curve adjusted in altitude so the $\dot{b} = 0$ point on the curve corresponded to the equilibrium line altitude (ELA) estimated for the glacier for that particular year. This procedure is based on the assumptions that the balance-altitude gradient for Muir Glacier was the same as that for McCarty Glacier and that the balance-altitude gradient remained reasonably constant in time for the periods considered. Neither assumption is entirely correct, but without data to develop more valid $\dot{b}(z)$ functions for different years or different glaciers, the ELA-adjusted McCarty $\dot{b}(z)$ curve was used as the best approximation. Although this procedure provides only a crude estimate, it is useful for the rapidly retreating glaciers considered here because Q_b is small compared with Q_h; values of Q_b range from 2 to 14 percent of the corresponding values of Q_h for the

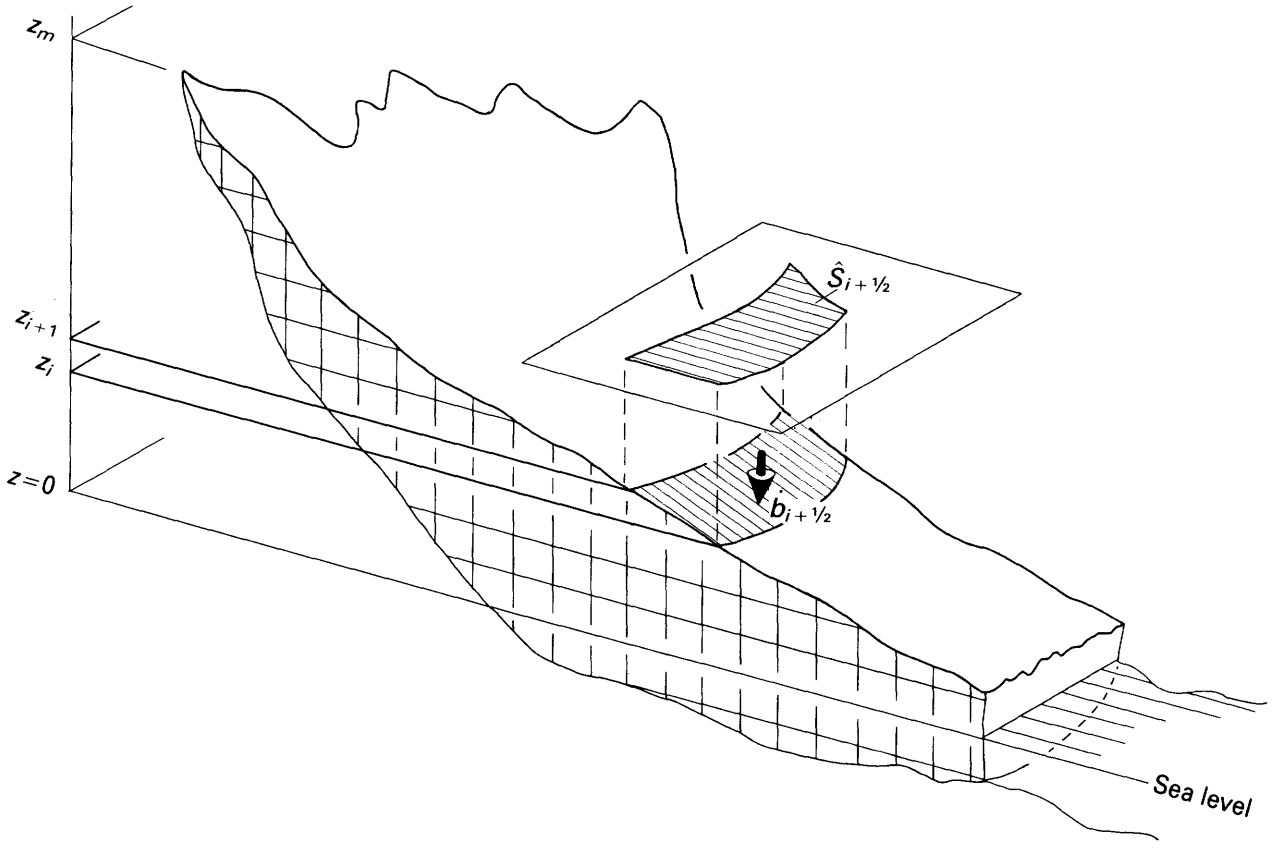

FIGURE 3.—Method of performing summation of balance flux (equation 6) where z is a vertical coordinate positive upward, $\hat{S}_{i+1/2}$ is the area of a vertical projection of the glacier surface, and $\dot{b}_{i+1/2}$ is the balance rate.

cases considered in this paper. Thus, the estimation of Q_b provides a small correction to the total flux.

The average thickness change flux, Q_h, is determined from the change in volume of the glacier averaged over the time interval T:

$$Q_h = -(V_T - V_0)/T \tag{7}$$

where V_T and V_0 are the volumes of the glacier at $t=0$ and $t=T$. The change in volume above h_g is obtained by summing the average of the areas between a contour line z_i and a contour line $z_i+\Delta z$ at $t=0$ and $t=T$, multiplied by Δz, a constant altitude interval (Finsterwalder, 1954):

$$V_T - V_0 = -\frac{1}{2}\sum_{i=1}^{n-1} (S'_i + S'_{i+1})\Delta z \tag{8}$$

where z_n is the highest altitude at which thinning occurred and S'_i is the area between z_i at $t=0$ and z_i at $t=T$ (fig. 4). The contour interval Δz, which is generally 500 ft (153 m), is adjusted for the lowest altitude interval because h_g usually does not fall on an even contour interval. Because this procedure does not take into account the volume loss from sea level to the top of the ice cliff or the volume loss below sea level, these volume losses must be calculated separately. The loss between $0<z<h_g$ is simply a special case of the above, and equation 8 was used with $\Delta z = h_g$. To calculate the loss below sea level (the exposed fiord), the average of several cross-sectional areas of the fiord exposed during the retreat in time T is multiplied by the known retreat distance. Plates 2C and D, 3B, C, and D, and 4A and B illustrate the changes in the sizes of the glaciers during the periods considered. Plates 2B, 3B, and 4A show the glaciers at their $t=T$ position and bathymetry out to the terminus positions at $t=0$. Table 6 gives the values for the variables Q_b, Q_h, $\bar{h}_w$, $\bar{h}_g$, and $\dot{\bar{X}}$ and the resulting value of $\bar{v}_c$.

Analysis of McCarty and Muir Glaciers during times of rapid retreat extends the range of calving results but not to the maximum calving speeds expected as Columbia Glacier recedes in future years. A data point in the range of very high calving speeds was estimated for the period 1860–79 in western Glacier Bay. Botanical studies indicate that ice retreated from the shore at Tlingit Point (pl. 4A) at about 1860 (Lawrence, 1958). At that time, the huge glacier occupying Glacier Bay was in

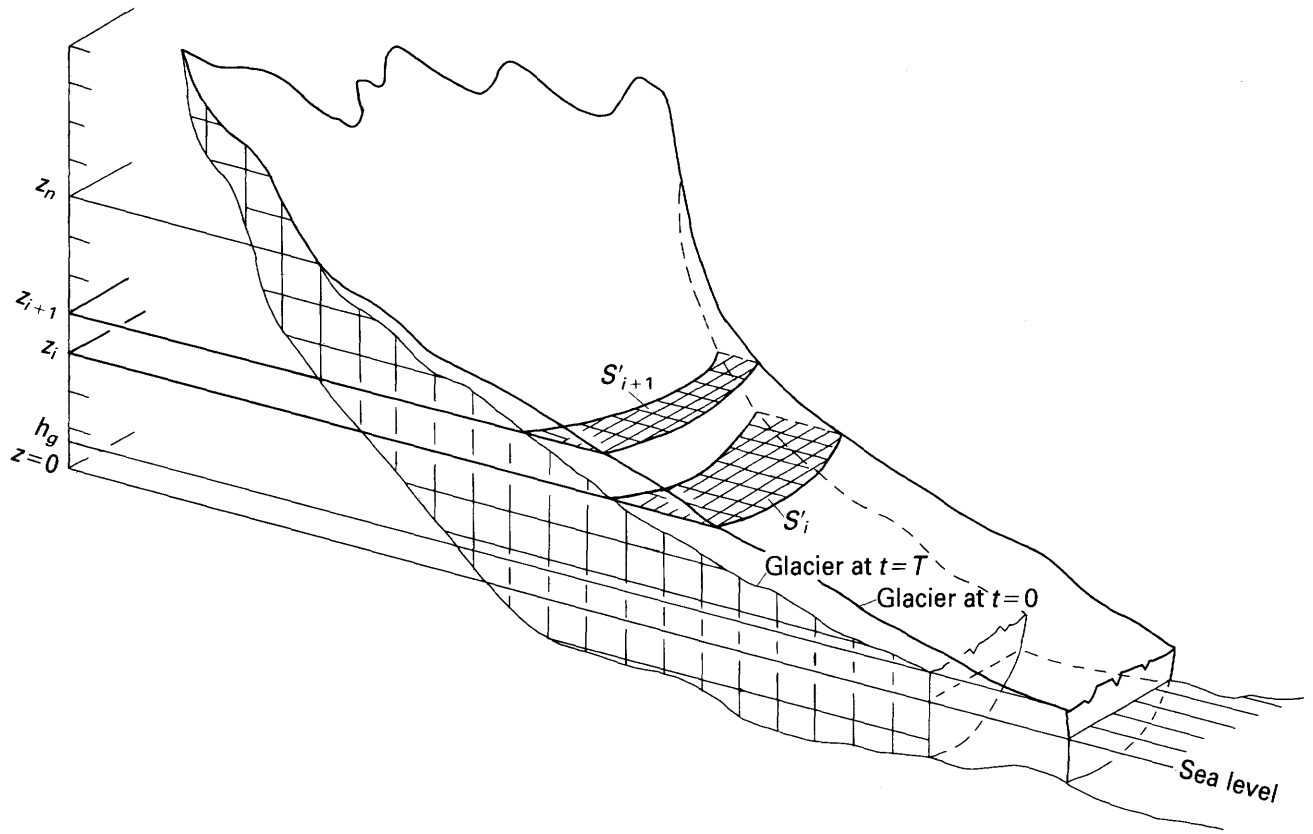

FIGURE 4.—Summation procedure of volume change (equation 8) where z is a vertical coordinate upwards, h_g is the ice cliff height, S' is the area between a given contour line at $t=0$ and $t=T$, T is the total time period of observation, and t is time.

very rapid retreat, and so the actual terminus was probably a deep embayment extending several kilometers upstream. Tlingit Point is 66 km from the assumed ice divide north of the United States-Canada boundary. Lawrence (1958, fig. 6) mapped the 1860 terminus with a deep embayment extending back to 56 km; Field (Bohn, 1967, p. 107) showed a less extreme embayment to 62 km. Because of this uncertainty, we consider that the probable location of the 1860 terminus was between the limits of 55 km (designated 1860 minimum) and 65 km (designated 1860 maximum).

As the ice in Glacier Bay retreated past Tlingit Point, it divided into two glacier systems, one to the east that retreated up Muir Inlet and one to the west that retreated up the western part of Glacier Bay, eventually into Tarr Inlet (Grand Pacific Glacier). For this report, we term the latter glacier system the west Glacier Bay glacier.

In 1879, John Muir (1915) described the terminus of the west Glacier Bay glacier at Russell Island, which located it at 28 ± 0.5 km. Thus, the average recession rate from 1860 to 1879 was between 1.97 and 1.40 km/a.

Detailed bathymetric soundings have been performed in this area, and so water depth is known. A balance-altitude function for west Glacier Bay was estimated from the McCarty balance-altitude function by using the same ELA-adjusted procedure as for Muir Glacier and the same assumptions. To estimate the balance and thickness-change fluxes, the centerline ice thickness must be estimated.

The shear stress, τ, at the bed of a glacier is given approximately by

$$\tau = s\rho_i g h \sin\alpha \tag{9}$$

where s is a shape factor ($0.5 < s < 1.0$), ρ_i is the density of ice, g is the acceleration of gravity, h is the ice thickness, and α is the surface slope. For most glaciers, $\tau \approx 1$ bar; τ is frequently assumed to be constant to estimate the dynamics of unmeasured glaciers (Budd and Jensen, 1975). Consider a coordinate x' measured upstream from the terminus; then $x' = X - x$. The base of west Glacier Bay glacier is virtually horizontal, and the surface slope angles are small, so that

$$\sin\alpha \approx \frac{dh}{dx'}. \tag{10}$$

We define

$$\mu \equiv s\rho_i g. \tag{11}$$

Assuming τ and μ to be constant with x,

$$\frac{\tau}{\mu} = h\frac{dh}{dx'} = \frac{1}{2}\frac{d(h^2)}{dx'}. \tag{12}$$

Therefore,

$$h^2(x') = \left(\frac{2\tau}{\mu}\right)x' + \text{constant}. \tag{13}$$

Transforming to a coordinate x measured downstream from the head of a glacier and setting $h = h_X$ at the terminus where $x = X$, the constant is evaluated, and equation 13 becomes

$$h^2(x) = \frac{2\tau}{\mu}(X - x) + h_X^2. \tag{14}$$

Thus, a profile can be constructed, assuming that μ, τ, and h_X are known. By adding a typical ice cliff height for a rapidly retreating large calving glacier ($60 < h_X < 100$ m) to the known water depth, h_X can be estimated; s probably lies between 0.8 and 0.9 for a large wide glacier such as this; ρ_i and g are known. Estimated value of τ is 1.0 bar. Coincidentally, the average τ calculated from the known thicknesses of Muir Glacier (east Glacier Bay) in 1892 and 1948 is 1.00 bar. Thus, the 1860 minimum, 1860 maximum, and 1879 centerline longitudinal profiles could be constructed (fig. 5). From these profiles, contour lines are extended to either side to form topographic maps (pl. 4A and B), from which the balance and thickness-change fluxes are estimated by integrating over altitude using equations 6 and 8 (table 6).

FORM OF THE CALVING LAW

An intuitive consideration of the stress distribution in the ice at the terminus of a calving glacier suggests that the calving speed may be a function of some combination of the variables h_g, h_w, and h, evaluated on the centerline or averaged over the width. One combination of interest is the ice thickness not supported by buoyancy, $h_u = h - \rho_w h_w/\rho_i$. The calving law is assumed to have the general form

$$v_c = f(\Phi) \tag{15}$$

where $\Phi \equiv h$, h_w, h_u, or h_g, or a combination of these, evaluated on the centerline or averaged over the width.

The possibility that calving is influenced by other variables such as accumulated strain, ice speed, water temperature, or state of the tide cannot be discounted. However, for Alaska glaciers, there is no direct evidence that these variables need to be separated explicitly. Studies at Columbia Glacier show that calving events are statistically uncorrelated with state of tide. However, there is evidence that subglacial runoff affects calving (discussed later in this section).

A number of possible forms of equation 15 were tested against the data shown in tables 1 and 6 by calculating

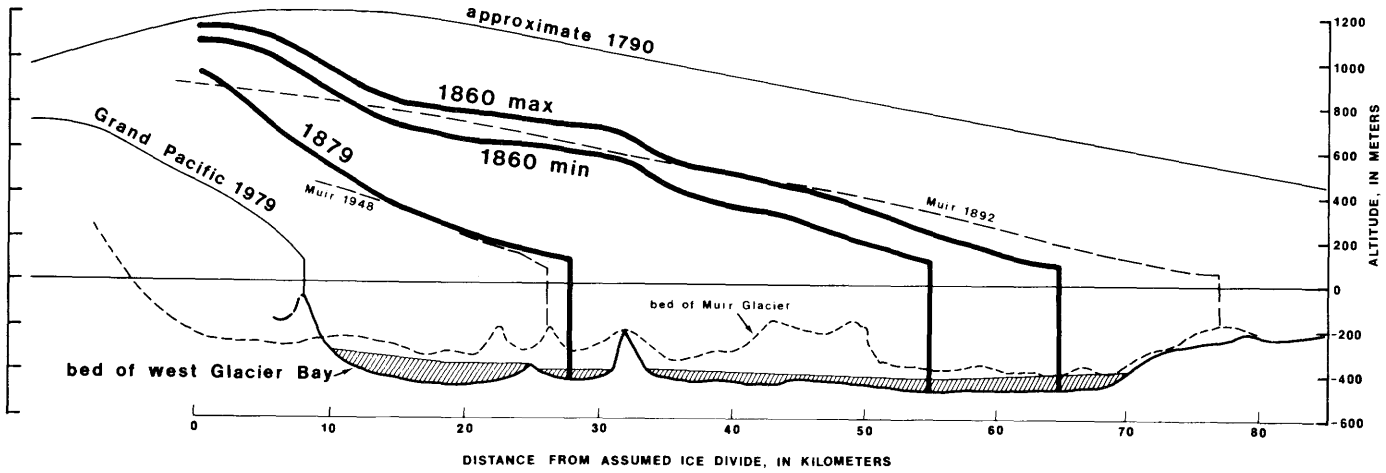

FIGURE 5.– Longitudinal surface and bed profiles of the west Glacier Bay glacier in 1860 (maximum), 1860 (minimum), 1879, and 1979. Shown for comparison are the longitudinal surface and bed profiles of Muir Glacier in 1892 and the approximate profile of the Glacier Bay glacier at its maximum extent preceding the historic 1790 retreat. Shaded area is the estimated thickness of sediment deposited on the bed of the west Glacier Bay since the glacier's retreat.

TABLE 6.–*Calving law data for those glaciers with no velocity measurements. Balance flux* Q_b *and thickness change flux* Q_h *for the entire glacier. Water depth,* $\bar{h}_w$*; ice surface height,* $\bar{h}_g$*; rate of advance,* $\dot{\bar{X}}$*; and calving speed,* $\bar{v}_c$ *averaged across the width at the terminus*

[Values given above; standard error given in parentheses below. Standard error determined or estimated from precision and density of measurements and possible lack of synchronism between measurements]

Number	Glacier	Time interval	Q_b ($\times 10^9 m^3/a$)	Q_h ($\times 10^9 m^3/a$)	$\bar{h}_w$ (m)	$\bar{h}_g$ (m)	$\dot{\bar{X}}$ (m/a)	$\bar{v}_c$ (m/a)
1a	McCarty	1942–1950	0.06	1.34	172	48	–1,220	4,200
			(.003)	(.07)	(5)	(5)	(25)	(1,100)
11a	Muir	1892–1948	0.07	2.07	180	68	–450	3,500
			(.02)	(.30)	(5)	(4)	(9)	(950)
11b	Muir	1948- 1972	0.03	1.21	173	64	–380	4,020
			(.02)	(.18)	(2)	(3)	(8)	(1,100)
13a	West Glacier Bay	1860 (min)–1879	–2.10	14.8	308	60	–1,400	9,400
			(.85)	(3)	(30)	(30)	(200)	(3,000)
13b	West Glacier Bay	1860 (max)–1879	–2.10	18.8	277	60	–1,950	12,500
			(.85)	(4)	(28)	(30)	(300)	(4,000)

F, a measure of the goodness of fit, and, in some cases, by calculating σ_c, the standard error of estimate of the coefficient c. The statistical measure, F, is the variance reduction fraction

$$F = 1 - \frac{\sum_i (v_c - \hat{v}_c)^2}{\sum_i (v_c - \langle v_c \rangle)^2} \tag{16}$$

where $\hat{v}_c$ is the value predicted by the relation, $\langle v_c \rangle$ is the mean observed value, and the sums are over the observed v_c of tables 1 and 6. For those two parameter formulas equivalent to linear regressions (such as $v_c = ch_w + d$ or $v_c = ch_w^p$), F is equivalent to r^2, the coefficient of determination. For some cases, the coefficient c and statistical measures σ_c and F are calculated with weighted data from tables 1 and 6, in which the weight is $[c^2 e_h^2 + e_v^2]^{-1}$ where e_h is the standard error in h or h_w and e_v is the standard error in v_c. In this calculation of weighting factors, c is the value determined from unweighted variables. No attempt was made to obtain a more correct value of c by iteration because the weighted and unweighted values were similar. Units of c assume v_c in meters per year and h and h_w in meters. The results are shown in table 7.

Surprisingly, one of the simplest of the possible calving relations

$$\bar{v}_c = c\bar{h}_w \tag{17}$$

gives an excellent fit to the data (fig. 6*A*) with a goodness of fit of 0.91 for the directly measured glaciers or 0.89 for the total set. The best estimate of the coefficient c is $27.1 \pm 2\ a^{-1}$. The power-law regressions and a logarithmic plot (fig. 6*B*) show that the best-fit relation is very close to linear, and the two-variable linear relation

TABLE 7. – *Calving relation forms and coefficients fitted to the data given in tables 1 and 6. Also given is the standard error of estimate of the coefficient σ_c and the variance reduction fraction* F (see page 9).

Calving relation forms	Coefficients	Directly measured glaciers (Glaciers from table 1) Unweighted	Directly measured glaciers (Glaciers from table 1) Weighted	All glaciers (Glaciers from tables 1 and 6) Unweighted	All glaciers (Glaciers from tables 1 and 6) Weighted
$\bar{v}_c = c\bar{h}_w$	c	24.4	28.0	27.9	27.1
	F	.69	.91	.81	.89
	σ_c	2.25	1.71	2.01	1.95
$\bar{v}_c = ch_w$	c	18.4	17.0	19.8	16.9
	F	.77	.85	.81	.84
	σ_c	1.46	1.10	1.47	.99
$\bar{v}_c = ch_w + d$	c	16.5		20.1	
	d	258		−84	
	F	.78		.81	
$\bar{v}_c = ch_w^p$	c	23		23.3	
	p	.95		.95	
	F	.73		.79	
$\bar{v}_c = ch$	c	11.8	8.38	14.3	9.08
	F	.77	.68	.74	.68
	σ_c	.98	.65	1.22	.70
$\bar{v}_c = ch^p$	c	1.14		1.66	
	p	1.42		1.36	
	F	.72		.75	
$\bar{v}_c = c(2h - h_w)$	c	8.18		10.97	
	F	.61		.65	
	σ_c	.69		1.42	
$\bar{v}_c = ch_w/h$	c	2.97×10^3		4.02×10^3	
	F	.56		.38	
	σ_c	336		578	
$v_c = ch_u$	c	104×10^3		140×10^3	
	F	−.44		−.14	
$\bar{v}_c = c\bar{h}_u$	c	79×10^3		117×10^3	
	F	−.35		.16	
$v_c = ch_u^p$	c	422		3.79×10^3	
	p	.38		−.10	
	F	.03		.002	
$\bar{v}_c = c\bar{h}_u^p$	c	218		15.1×10^3	
	p	.48		−.53	
	F	.03		.04	
$v_c = ch_u^{-2.18}$	c	5.52×10^6		6.97×10^6	
	F	−1.27		−.62	
$\bar{v}_c = ch_u^{-2.18}$	c	4.26×10^6		6.45×10^6	
	F	−1.10		−.01	
$v_c = cA^{0.569}h_u^{-2.18}$	c	58.9		107.6	
	F	−1.48		−.3	

shows that calving is approximately zero when the water depth is zero, further supporting the simple one-coefficient, one-independent-variable calving relation of equation 17. Figures 6*A* and *B* also show that equation 17 applies to Columbia Glacier within the margin of error.

Sikonia and Post (1979) showed that calving rates measured over a few weeks or months at the head of an embayment at Columbia Glacier appeared to be related to short-term variations in runoff as observed qualitatively at the terminus. Sikonia (1982) utilized a three-coefficient calving relation of the form

$$v_c = cD^p h_u^q \tag{18}$$

where h_u is measured at the head of the calving embayment and D is the short-term runoff at the terminus, assumed to be proportional to the runoff of the glacial stream Knik River near Palmer, Alaska. The best-fit

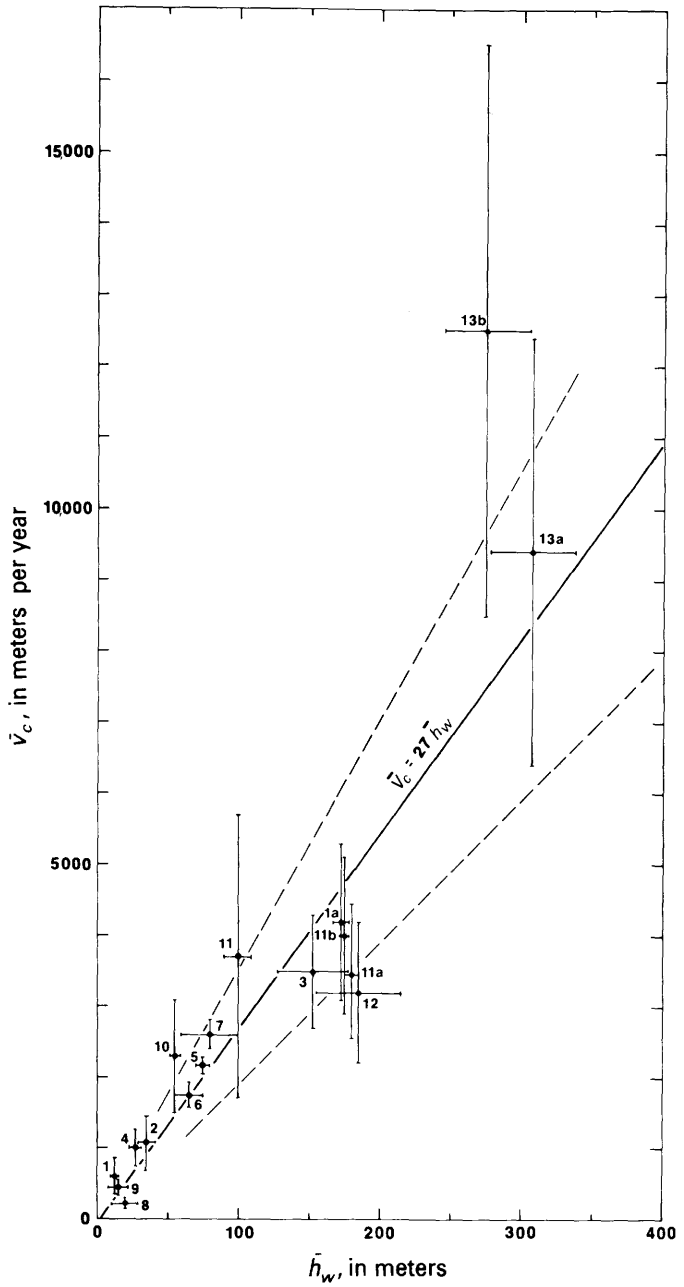

FIGURE 6A.—Linear plot of calving speed $\bar{v}_c$ as a function of mean water depth, $\bar{h}_w$. The glaciers are numbered as in tables 1 and 6; error bars for both calving speed and water depth refer to known or estimated standard errors. Also shown are the mean regression line (solid) and 95-percent confidence limits (dashed lines) for a calving relation of the form $\bar{v}_c = c\bar{h}_w$.

values of the coefficients were $c = 1.09 \times 10^6$, $p = 0.57$, and $q = -2.18$, where units of D are m^3/s. This relation could not be tested directly against data from other glaciers.

Sikonia (1982) tested the simple annual-averaged and width-averaged calving relation (eq. 17) on short-term rates of calving at the head of the embayment of Columbia Glacier and found virtually no fit to the data ($r^2 = 0.08$). Thus, this calving relation does not apply to short-term embayment calving. Conversely, applying the short-term embayment calving relation (eq. 18) to the data of tables 1 and 6, assuming constant but unknown discharge or discharge proportional to glacier area, yields virtually no fit to the data ($F < 0$), as shown in the last 3 forms in table 7. Thus, the seasonal short-term calving relation incorporating streamflow does not appear to apply to annually averaged data from other glaciers.

These calving relations do not apply to floating glaciers. If a glacier were to float, the calving speed calculated by equation 17 would increase with increasing depth of water under the glacier, which does not appear to be reasonable, and the calving speed calculated by equation 18 would be undetermined and would increase without bound because the exponent of h_u is negative. For the calving glaciers observed, the ratio of thickness necessary for flotation to actual thickness does not exceed 0.93, and, thus, none of them are floating; no floating glacier termini are known in Alaska at the present or in the recent past. Literature exists on the calving of floating ice sheets (for example, Reeh, 1968; Holdsworth, 1973), but the calving speed to be expected if one of the presently grounded Alaskan glaciers were to float is unknown. Certain floating termini of outlet glaciers in Greenland may be analogous; the fastest of these (Jacobshavn) has a centerline calving speed of about 7.5 km/a (Kollmeyer, 1980).

CONCLUSION

Although precise calculation of the rate of calving of a tidal glacier is a complex exercise, an approximation to the annual calving speed may be made by using only the water depth at the terminus. These water depth data are available for almost all the present and past tidal glaciers in Alaska. Thus, analyses of the variations of Alaskan calving glaciers can proceed in a more quantitative manner, and a very simple relation can be used as the terminus boundary condition for modeling these glaciers.

This empirical study also accentuates the need for more understanding of the physics of calving. Why, for instance, does short-term calving in embayments relate to different variables than those appropriate to width and annual averages of calving? The data reported in this paper should be useful for the further development and testing of calving theories and models.

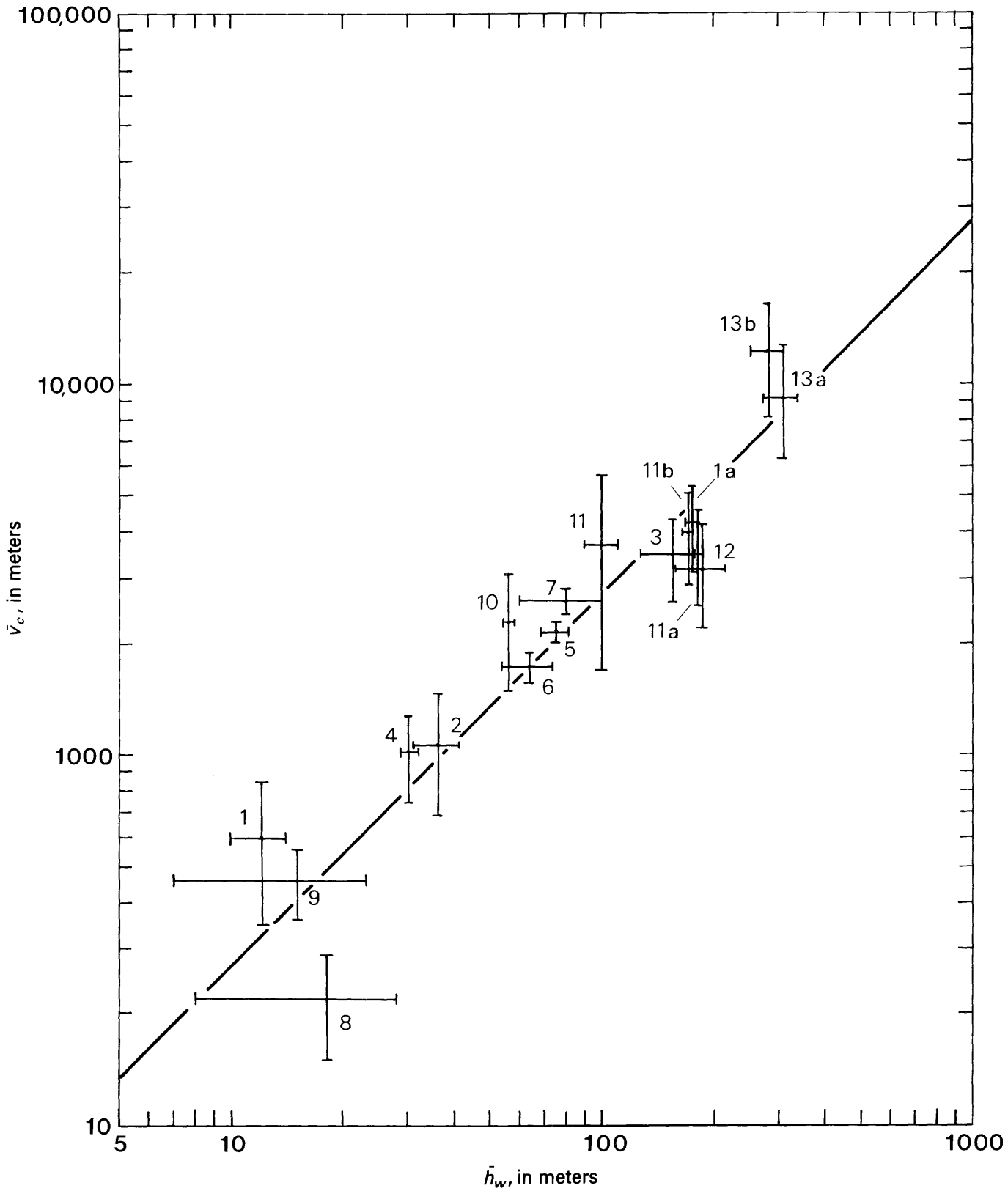

FIGURE 6B. – Logarithmic plot of $\bar{v}_c$ as a function of mean water depth, $\bar{h}_w$. The glaciers are numbered as in tables 1 and 6; error bars for both calving speed and water depth refer to known or estimated standard errors. Also shown is the mean regression line (solid) for a calving relation of the form $\bar{v}_c = c\bar{h}_w$.

REFERENCES CITED

Bohn, Dave, 1967, Glacier Bay: The land and the silence: Alaska National Parks and Monuments Association, 160 p.

Budd, W. F., and Jenssen, D., 1975, Numerical modelling of glacier systems: Proceedings of the Moscow Symposium, August 1971; Actes du Colloque de Moscou, aout 1971: IAHS-AISH Publication, no. 104, p. 257–291.

Field, W. O., 1947, Glacier recession in Muir Inlet, Glacier Bay, Alaska: The Geographical Review, American Geographical Society, v. 37, no. 3, p. 369–399.

Field, W. O., ed., 1975 (v. 2), Mountain glaciers of the Northern Hemisphere: Hanover, New Hampshire, Cold Regions Research and Engineering Laboratory, p. 299–492.

Finsterwalder, Richard, 1954, Photogrammetry and glacier research with special reference to glacier retreat in the eastern Alps: Journal of Glaciology, v. 2, no. 15, p. 306–312.

Holdsworth, Gerald, 1973, Ice calving into the proglacial Generator Lake, Baffin Island, N.W.T., Canada: Journal of Glaciology, v. 12, no. 65, p. 235–50.

Iken, Almut, 1977, Movement of a large ice mass before breaking off: Journal of Glaciology, v. 19, no. 81, p. 595–605.

Kollmeyer, R. C., 1980, West Greenland outlet glaciers: An inventory of the major iceberg producers, *in* World Glacier Inventory, Proceedings of the Riederalp Workshop, September 1978, IAHS-AISH Publication, no. 126, p. 57–64.

Lawrence, D. B., 1958, Glaciers and vegetation in southeastern Alaska: American Scientist, v. 46, no. 2, p. 89–122.

Meier, M. F., Post, Austin, Rasmussen, L. A., Sikonia, W. G., and Mayo, L. R., 1980a, Retreat of Columbia Glacier–a preliminary prediction: U.S. Geological Survey Open-File Report 80–10, 9 p.

Meier, M. F., Rasmussen, L. A., Post, Austin, Brown, C. S., Sikonia, W. G., Bindschadler, R. A., Mayo, L. R., and Trabant, D. C., 1980b, Predicted timing and disintegration of the lower reach of Columbia Glacier, Alaska: U.S. Geological Survey Open-File Report 80–582, 47 p.

Muir, John, 1915, Travels in Alaska: Houghton Mifflin, Boston, 327 p.

Post, Austin, 1975, Preliminary hydrography and historic terminal changes of Columbia Glacier, Alaska: U.S. Geological Survey Hydrologic Investigations Atlas 559, 3 sheets.

———1980a, Preliminary bathymetry of Northwestern Fiord and neoglacial changes of Northwestern Glacier, Alaska: U.S. Geological Survey Open-File Report 80–414, 2 sheets.

———1980b, Preliminary bathymetry of Blackstone Bay and neoglacial changes of Blackstone Glacier, Alaska: U.S. Geological Survey Open-File Report 80–418, 2 sheets.

———1980c, Preliminary bathymetry of Aialik Bay and neoglacial changes of Aialik and Pederson Glaciers, Alaska: U.S. Geological Survey Open-File Report 80–423, 1 sheet.

———1980d, Preliminary bathymetry of McCarty Fiord and neoglacial changes of McCarty Glacier, Alaska: U.S. Geological Survey Open-File Report 80–424, 4 sheets.

———1980e, Preliminary bathymetry–Esther Passage to Eaglek Island, Alaska: U.S. Geological Survey Open-File Report 80–426, 1 sheet.

———1980f, Preliminary bathymetry–approaches to Unakwik Inlet, Alaska: U.S. Geological Survey Open-File Report 80–428, 1 sheet.

Rasmussen, L. A. and Meier, M. F., 1982, A continuity equation model of the drastic retreat of Columbia Glacier, Alaska: U.S. Geological Survey Professional Paper 1258–A.

Reeh, Niels, 1968, On the calving of ice from floating glaciers and ice shelves: Journal of Glaciology, v. 7, no. 50, p. 215–32.

Reid, H. F., 1896, Glacier Bay and its glaciers: U.S. Geological Survey Sixteenth Annual Report, pt. 1, p. 415–461.

Sikonia, W. G., 1982, A two-dimensional dynamic finite-element glacier flow model applied to Columbia Glacier, Alaska: U.S. Geological Survey Professional Paper 1258–B.

Sikonia, W. G., and Post, Austin, 1979, Columbia Glacier, Alaska: Recent ice loss and its relationship to seasonal terminal embayments, thinning, and glacier flow: U.S. Geological Survey Open-File Report 79–1265, 2 sheets.

☆U.S. GOVERNMENT PRINTING OFFICE:1983-381-614/191